Advances in Nano Research, *Vol. 16, No.6 (2024) 565-577*
https://doi.org/10.12989/anr.2024.16.6.565

Fluid bounding effect on FG cylindrical shell using Hankel's functions of second kind

Khaled Mohamed Khedher*[1], Shahzad Ali Chattah[2], Mohammad Amien Khadimallah[3], Ikram Ahmad[4], Muzamal Hussain[5], Rana Muhammad Akram Muntazir[6], Mohamed Abdelaziz Salem[7], Ghulam Murtaza[5], Faisal Al-Thobiani[8], Muhammad Naeem Mohsin[9], Abeera Talib[6] and Abdelouahed Tounsi[10,11]

[1]*Department of Civil Engineering, College of Engineering, King Khalid University, Abha 61421, Saudi Arabia*
[2]*Department of Chemistry, Government College University Faisalabad, 38000, Pakistan*
[3]*Department of Civil Engineering, College of Engineering in Al-Kharj, Prince Sattam Bin Abdulaziz University, Al-Kharj, 11942, Saudi Arabia*
[4]*Department of Chemistry, University of Sahiwal, Sahiwal, 57000, Faisalabad, Pakistan*
[5]*Department of Mathematics, University of Sahiwal, Sahiwal, 57000, Faisalabad, Pakistan*
[6]*Department of Mathematics, Lahore leads University, 54792, Lahore*
[7]*Department of Mechanical Engineering, College of Engineering, King Khalid University, Abha 61421, Saudi Arabia*
[8]*Marine Engineering Department, Faculty of Maritime Studies, King Abdulaziz University, Jeddah, Saudi Arabia*
[9]*Institute for Islamic Theological Studies, University of Vienna, Schenkenstrabe 8-10,1010, Vienna*
[10]*Faculty of Technology Civil Engineering Department, Materials and Hydrology Laboratory University of Sidi Bel Abbes, Algeria*
[11]*Department of Civil and Environmental Engineering, King Fahd University of Petroleum and Minerals, 31261 Dhahran, Eastern Province, Saudi Arabia*

(*Received July 22, 2021, Revised May 3, 2024, Accepted May 5, 2024*)

Abstract. Vibration investigation of fluid-filled functionally graded cylindrical shells with ring supports is studied here. Shell motion equations are framed first order shell theory due to Sander. These equations are partial differential equations which are usually solved by approximate technique. Robust and efficient techniques are favored to get precise results. Employment of the Rayleigh-Ritz procedure gives birth to the shell frequency equation. Use of acoustic wave equation is done to incorporate the sound pressure produced in a fluid. Hankel's functions of second kind designate the fluid influence. Mathematically the integral form of the Langrange energy functional is converted into a set of three partial differential equations. A cylindrical shell is immersed in a fluid which is a non-viscous one. These shells are stiffened by rings in the tangential direction. For isotropic materials, the physical properties are same everywhere where the laminated and functionally graded materials, they vary from point to point. Here the shell material has been taken as functionally graded material. After these, ring supports are located at various positions along the axial direction round the shell circumferential direction. The influence of the ring supports is investigated at various positions. Effect of ring supports with empty and fluid-filled shell is presented using the Rayleigh - Ritz method with simply supported condition. The frequency behavior is investigated with empty and fluid-filled cylindrical shell with ring supports versus circumferential wave number and axial wave number. Also the variations have been plotted against the locations of ring supports for length-to-radius and height-to-radius ratio. Moreover, frequency pattern is found for the various position of ring supports for empty and fluid-filled cylindrical shell. The frequency first increases and gain maximum value in the midway of the shell length and then lowers down. It is found that due to inducting the fluid term frequency result down than that of empty cylinder. It is also exhibited that the effect of frequencies is investigated by varying the surfaces with stainless steel and nickel as a constituent material. To generate the fundamental natural frequencies and for better accuracy and effectiveness, the computer software MATLAB is used.

Keywords: fluid-filled; Hankel's functions; MATLAB; Sender's shell theory; strain energy

1. Introduction

Vibration fluid-filled shell problems occur in industrial engineering fields. Their vibration analysis predicts to approximate their experimental results. Nature of a shell material plays an important role in specifying their vibration frequencies. Stability of a cylindrical shell depends highly on these aspects of material. More the shell material sustains a load due to physical situations, the more the shell is stable. Any predicted fatigue due to burden of vibrations is evaded by estimating their dynamical aspects. Study of vibration characteristics of fluid-filled cylindrical shells is a widely area of research in applied mathematics, theoretical mechanics and nano-fluids (Dong *et al*. 2024, Sun *et al*. 2023, 2024, Zhu *et al*. 2023) and nano-particles (Long *et al*. 2023, Yang *et al*. 2023). Analytical investigation of vibrations of these shell are performed to estimate the probable dynamical response.

Variations in the shell physical parameters are inducted to enhance their strength and stability. Addition of more physical parameters may give rise more instability in a system of a submerged cylindrical shell (CSs). During the recent years, study of submerged cylindrical shell has gained the attention of researchers doing work on their

*Corresponding author, Professor, Ph.D.,
E-mail: kkhedher@kku.edu.sa

ISSN: 2287-237X (Print), 2287-2388 (Online)

vibration characteristics. Advanced composite materials keep extreme particular stiffness, strength and are resistant to corrosion (Kuang *et al*. 2018, Cao *et al*. 2022, Zhu *et al*. 2017, Zhu *et al*. 2017). The acoustic wave equation is applied to extract influence of a fluid on shell vibrations. Firstly, Love (1888) presented the Kirchhoff's hypotheses for plates. After that this theory became a foundation stage for building new ones by changing physical terms expressions.

More than one type of materials is used to structure the functionally graded (FG) materials and their physical properties vary from one surface to the other surface. In these surfaces, one has highly heat resistance property while other may preserve great dynamical perseverance and differs mechanically and physically in regular manner from one surface to other surface, making them of dual physical appearance. All these materials have changeable outer and inner sides and their physical properties greatly differ from each other (Suresh and Mortensen 1997, Koizumi, 1997). These materials are organized by various techniques and their applications are seen in dynamical elements such as plates, beams and shells. Moreover, they are also observed in space crafts, nuclear reactors and missiles technology etc. Loy and Lam (1997) investigated shell vibrations with ring supports that restricted the motion of cylindrical shells in the transverse direction. This influence was inducted by the polynomial functions. Xiang *et al.* (2002) formed some closed form solution functions for studying vibrations of cylindrical shells. The mid-way ring supports were clamped around the shells. Sewall and Naumann (1968) considered the vibration analysis of CSs based on analytical and experimental methods. The shells were strengthened with longitudinal stiffeners. Sharma (1974) analyzed vibration frequencies circular cylinder with using the Rayleigh - Ritz formulation and made comparisons of his results with some experimental ones. Chung *et al.* (1981) investigated the vibrations of fluid-filled CSs and presented an analysis of experimental and analytical investigation. Goncalves and Batista (1987) gave an analytical investigation of CSs partially filled and submerged in a fluid.

Jiang and Olson (1994) recommended the characteristics of analysis of stiffened shell using finite element method to diminish large computational efforts which are required in the conventional finite element analysis. Wang *et al*. (1997) scrutinized the vibrations of ring-stiffened CSs using Ritz polynomial functions. Materials of both shells and rings were of isotropic nature. These shells were stiffened with isotropic rings having three types of locations on the shell outer surface. To increase the stiffness of CSs was stabilized by ring-stiffeners. Isotopic materials are the constituents of these rings. A large use of shell structures in practical applications makes their theoretical analysis an important field of structural dynamics. Since a shell problem is a physical one, so their vibrational behaviors are distorted by variations of physical and material parameters. To elude any complications which may risk a physical system their analytical investigation was done. Sharma *et al*. (1998) determined frequencies of composite cylindrical shells containing fluid. They estimated the axial modal deformations by trigonometric functions. Ergin and Temarel (2002) did a vibration study of cylindrical shells. The shells lied in a horizontal direction and contained fluid and submerged in it. Zhang (2002) studied vibrations of CSs submerged in a fluid. It was seen that the fluid factor impressed vibration shell frequencies to a significant limit. Najafizadeh and Isvandzibaei (2007) applied ring supports to CSs for vibration analysis of along the tangential direction and founded their research on angular deformation theory of higher order. The angular deformation was used for shell equations and determined the effects of constituent volume fractions and shell configurations on the shell vibrations. FG material parameters were changed step by step. Shah *et al*. (2009) and Sofiyev and Avcar (2010) studied stability of CSs based on Rayleigh - Ritz (RRM) and Galerkin technique using elastic foundations. The structures of cylindrical shell are tackled under the exponential law and axial load. Naeem *et al*. (2013) conducted the vibrational behavior of submerged FG-CSs. The problem of submerged cylindrical shells were frequently met where fluid envelopes a structure. The present problem consists of a cylindrical shell submerged in a fluid and surrounded by ring supports. There is no evidence found where this problem has not been studied earlier. Ansari *et al*. (2015) performed nonlocal model for the frequencies of multi-walled carbon nanotubes with small effects subject to various boundary conditions (BCs) using Rayleigh-Ritz technique. The governing equation was formulated based on Flügge's and nonlocal shell theory. Some new resonant frequencies were identified with the association of vibrational modes and circumferential modes into shell model. Pankaj *et al*. (2019) studied the functionally graded material using sigmoid law distribution under hygrothermal effect. The Eigen frequencies are investigated in detail. Frequency spectra for aspect ratios have been depicted according to various edge conditions. Recently some researcher used different methods for nonlinear modeling (Tohidi *et al*. 2018, Zhang *et al*. 2024, Arefi and Zenkour 2017, Yang *et al*. 2022, Arani*et al*. 2018, Wang *et al*. 2023a, b, Krommer *et al*. 2016, Liu *et al*. 2024, Yeh, 2016, Taj *et al*. 2021, Iqbal *et al*. 2021, Alwabli *et al*. 2021, Taj *et al*. 2020). Recently some researcher used different methods for nonlinear modeling (Eltaher *et al.* 2019, Li *et al*. 2020, 2023, Ebrahimi *et al.* 2019, Safaei *et al.* 2019, Shahsavari *et al.* 2019, Han *et al*. 2018 Benmansour *et al.* 2019, Sobamowo *et al*. 2017, Guo *et al.* 2023, Sedighi *et al*. 2020, Gong *et al*. 2024, Mousavi *et al*. 2021, Fu *et al*. 2020, 2024, Sedighi 2020, Dang *et al*. 2021, Akbaş 2016a, b, 2017a, b, Feng *et al*. 2024, Khadimallah *et al*. 2020a, b, Asghar *et al*. 2020a, b, Sharif *et al*. 2020, Iqbal *et al*. 2020).

According to our knowledge, up to now little is known about the vibration analyses of varying two different material and has not been investigated for fluid-filled FG-CS with ring supports based on Rayleigh-Ritz procedure. The proposed model is quite straightforward for the vibrational analysis of these structures of CSs. A large use of shell structures in practical applications makes their theoretical analysis an important field of structural dynamics. Since a shell problem is a physical one, so their vibrational behaviors are distorted by variations of physical

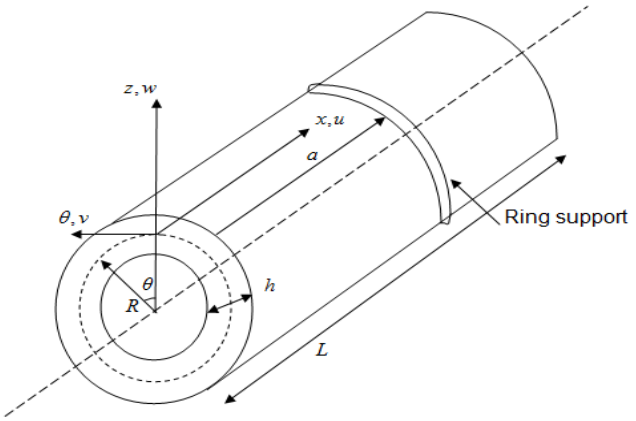

Fig. 1 Geometry of cylindrical shell with ring support

and material parameters. It is also exhibited that the effect of frequencies by varying the stainless steel and nickel as a constituent material. Also the Love shell model based on the wave propagation approach for estimating fundamental natural frequency has been developed to converge more quickly than other methods and models. The influence of the ring supports is investigated at various positions. Effect of ring supports with empty and fluid-filled shell is presented using the Rayleigh - Ritz method with simply supported condition. The frequency behavior is investigated with empty and fluid-filled cylindrical shell with ring supports versus circumferential wave number and axial wave number. Also the variations have been plotted against the locations of ring supports for length-to-radius and height-to-radius ratio. Moreover, frequency pattern is found for the various position of ring supports for empty and fluid-filled cylindrical shell. The frequency first increases and gain maximum value in the midway of the shell length and then lowers down. The presented vibration modeling and analysis of CSs may be helpful especially in applications such as oscillators and in non-destructive testing. To elude any complications which may risk a physical system their analytical investigation is done.

2. Theoretical formation

The geometrical parameters L, h, R denotes as length, thickness and radius for CSs with its coordinate system (x, θ, z) as shown in Fig. 1. The x, θ co-ordinate are assumed to be along longitudinal and circumferential direction, respectively and z - co-ordinates are taken in its radial directions.

When the material and geometrical parameters are considered, the formula for a strain energy, S of a vibrating cylindrical shell is expressed as (Loy and Lam 1997).

$$\begin{aligned} S = \frac{R}{2}\int_0^L\int_0^{2\pi} & [A_{11}\,e_1^2 + A_{22}e_2^2 + 2A_{12}e_1e_2 \\ & + A_{66}e_{12}^2 + 2\begin{pmatrix} B_{11}e_1k_1 + B_{11}e_1k_1 + B_{11}e_1k_1 \\ + B_{11}e_1k_1 + 2B_{66}e_{12}k_{12} \end{pmatrix} \\ & + D_{11}k_1^2 + D_{22}k_2^2 + 2D_{12}k_1k_2 + D_{66}^2k_{12}^2]d\theta dx \end{aligned} \quad (1)$$

where e_1, e_2, e_3 and k_1, k_2, k_3 designate the surface strains and curvatures respectively. The extensional stiffness, A_{ij}, coupling stiffness, B_{ij} and bending stiffness, D_{ij} are written as:

$$\{A_{ij}, B_{ij}, D_{ij}\} = \int_{-h/2}^{h/2} Q_{ij}\{1, z, z^2\}dz(i, j = 1,2,6) \quad (2)$$

Here the reduced stiffness, Q_{ij}'s are written as for isotropic CSs:

$$Q_{11} = Q_{22} = \frac{E}{1-v^2}\ ,\quad Q_{12} = \frac{vE}{1-v^2}\ ,\quad Q_{66} = \frac{E}{2(1+v)} \quad (3)$$

The strain-displacement relations from Budiansky and Sanders (1963) furnished as:

$$e_{12} = \frac{\partial y}{\partial x},\ e_{22} = \frac{1}{R}\left(\frac{\partial v}{\partial \theta} - w\right),\quad e_{12} = \frac{\partial v}{\partial x} + \frac{1}{R}\frac{\partial u}{\partial \theta} \quad (4)$$

and the expressions for the curvature - displacement relations are represented as:

$$\begin{aligned} k_{11} = \frac{\partial^2 w}{\partial x^2},\ k_{22} = \frac{1}{R^2}\left(\frac{\partial^2 w}{\partial \theta^2} + \frac{\partial v}{\partial \theta}\right), \\ k_{12} = \frac{1}{R}\left(\frac{\partial^2 w}{\partial x \partial \theta} + \frac{3}{4}\frac{\partial v}{\partial x} - \frac{1}{4R}\frac{\partial u}{\partial \theta}\right) \end{aligned} \quad (5)$$

expression (4) and (5) into the formula (1), the strain energy, S is takes the new forms:

$$\begin{aligned} S = \frac{1}{2}\int_0^{2\pi L}\int_0^{} & [A_{11}\left(\frac{\partial u}{\partial x}\right)^2 + A_{22}\frac{1}{R^2}\left(\frac{\partial v}{\partial \theta} + w\right)^2 \\ & + 2A_{12}\frac{1}{R}\frac{\partial u}{\partial x}\left(\frac{\partial v}{\partial \theta} + w\right) + A_{66}\left(\frac{\partial v}{\partial \theta} + \frac{1}{R}\frac{\partial u}{\partial x}\right)^2 \\ & - 2B_{11}\left(\frac{\partial u}{\partial x}\right)\left(\frac{\partial^2 w}{\partial x^2}\right) - 2B_{12}\frac{1}{R^2}\left(\frac{\partial u}{\partial x}\right)\left(\frac{\partial^2 w}{\partial \theta^2} - \frac{\partial v}{\partial \theta}\right) \\ & - 2B_{12}\frac{1}{R}\left(\frac{\partial v}{\partial \theta} + w\right)\left(\frac{\partial^2 w}{\partial x^2}\right) - 2B_{22}\frac{1}{R^3}\left(\frac{\partial v}{\partial \theta} + w\right)\left(\frac{\partial^2 w}{\partial \theta^2} - \frac{\partial v}{\partial \theta}\right) \\ & - 4B_{66}\frac{1}{R}\left(\frac{\partial v}{\partial \theta} + \frac{1}{R}\frac{\partial u}{\partial x}\right)\left(\frac{\partial^2 w}{\partial x \partial \theta} - \frac{3}{4}\frac{\partial v}{\partial x} + \frac{1}{4R}\frac{\partial u}{\partial \theta}\right) \\ & + D_{11}\left(\frac{\partial^2 w}{\partial x^2}\right)^2 + \frac{D_{22}}{R^4}\left(\frac{\partial^2 w}{\partial \theta^2} - \frac{\partial v}{\partial \theta}\right)^2 \\ & + 2D_{12}\frac{1}{R^2}\left(\frac{\partial^2 w}{\partial x^2}\right)\left(\frac{\partial^2 w}{\partial \theta^2} - \frac{\partial v}{\partial \theta}\right) \\ & + 4D_{66}\frac{1}{R^2}\left(\frac{\partial^2 w}{\partial x \partial \theta} - \frac{3}{4}\frac{\partial v}{\partial x} + \frac{1}{4R}\frac{\partial u}{\partial \theta}\right)^2]Rdxd\theta \end{aligned} \quad (6)$$

The shell kinetic energy, K of the cylindrical shell is written as:

$$K = \frac{1}{2}\int_0^{2\pi L}\int_0^{} \rho_t\left[\left(\frac{\partial u}{\partial t}\right)^2 + \left(\frac{\partial v}{\partial t}\right)^2 + \left(\frac{\partial w}{\partial t}\right)^2\right]Rdxd\theta \quad (7)$$

where ρ_t is designated as:

$$\rho_t = \int_{-h/2}^{h/2} \rho dz \quad (8)$$

The mass densityρ remains constant for an isotropic material. The Langrange energy functional $\prod$ for a vibrating cylindrical shell is stated as the difference between kinetic and strain energies and is expressed as:

$$\prod = K - S \quad (9)$$

3. Solution methodology

Here Rayleigh's method is engaged to solve the CSs problem of differential equations in an efficient and comprehensive way. This method needs the axial modal approximates dependence on the characteristic function. The governing equation was formulated based on Sander's thin shell theory with energy functional. In present work, the current method is used to find the vibration of FG-CSs. Over the past several years vibration of shell structures of various boundary conditions have been extensively studied (Wang *et al*. 1997). The RRM is very powerful technique for the prediction of vibration of shells. Axial, circumferential and radial direction is related only to the axial displacement function. The unknown functions involving the tube dynamical equations are functions of shape linear variables. The independent variables are separated by employing prescribed method. They are supposed in the form of the product of separate functions of independent variables.

$$\begin{aligned} u(x,\theta,t) &= A_m \frac{d\varphi}{dx} cos\, n\,\theta\, sin\,\omega\, t \\ v(x,\theta,t) &= B_m \varphi(x) \sin n\,\theta\, sin\,\omega\, t \\ w(x,\theta,t) &= C_m \varphi(x) \prod_{i=1}^{N} (x-a_i)^{\varepsilon_i} cos\, n\,\theta\, sin\,\omega\, t \end{aligned} \tag{10}$$

where A_m, B_m, C_m are taken as the displacement amplitudes in x, θ and z directions. The angular frequency and circumferential wave number are represented by ω and n respectivelywhere. The axial function $\varphi(x)$ represents axial modal displacement shapes and satisfies the geometric boundary conditions. The term $x = a_i$ is the i^{th} ring supports along longitudinal direction and *N*, ε_i designates for number and existence of ring supports. When there is no ring on the shell the condition is $\varepsilon_i = 0$ and for ring supports is $\varepsilon_i = 1$.

The modified form of strain and kinetic energy with axial displacement functions:

$$\begin{aligned} U = \frac{\pi R}{2}\int_0^L [& A_{11} A_m^2 \frac{d^2\varphi}{dx^2} + \frac{A_{22}}{R^2}\{nB_m\varphi + C_m\varphi(x-a)\}^2 \\ & + \frac{2A_{12}}{R}\left(A_m \frac{d^2\varphi}{dx^2}\right)\{nB_m\varphi + C_m\varphi(x-a)\} \\ & + A_{66}(B_m \frac{d\varphi}{dx} - \frac{nA_m}{R}\frac{d\varphi}{dx})^2 \\ & - 2B_{11}\left(A_m \frac{d^2\varphi}{dx^2}\right)\left\{C_m\left(\frac{d^2\varphi}{dx^2}(x-a) + 2\frac{d\varphi}{dx}\right)\right\} \\ & - \frac{2B_{12}}{R^2}\left(A_m \frac{d^2\varphi}{dx^2}\right)\{-n^2 C_m\varphi(x-a) - nB_m\varphi\} \\ & - \frac{2B_{12}}{R}\{nB_m\varphi + C_m\varphi(x-a)\}\left\{C_m\left(\frac{d^2\varphi}{dx^2}(x-a) + 2\frac{d\varphi}{dx}\right)\right\} \\ & - \frac{2B_{22}}{R^3}\{nB_m\varphi + C_m\varphi(x-a)\}\{-n^2 C_m\varphi(x-a) - nB_m\varphi\} \\ & - \frac{4B_{66}}{R}\left\{B_m \frac{d\varphi}{dx} - \frac{nA_m}{R}\frac{d\varphi}{dx}\right\}\begin{Bmatrix} -nC_m\left(\frac{d\varphi}{dx}(x-a) + \varphi\right) \\ -B_m \frac{d\varphi}{dx} \end{Bmatrix} \\ & + D_{11}\{C_m(\frac{d^2\varphi}{dx^2}(x-a) + 2\frac{d\varphi}{dx})\}^2 \frac{D_{22}}{R^4}\{-n^2 C_m\varphi(x-a) \\ & \qquad - nB_m\varphi\}^2 \end{aligned} \tag{11}$$

$$\begin{aligned} & + \frac{2D_{12}}{R^2}\left\{C_m\left(\frac{d^2\varphi}{dx^2}(x-a) + 2\frac{d\varphi}{dx}\right)\right\}\{-n^2 C_m\varphi(x-a) \\ & \qquad - nB_m\varphi\} \\ & + \frac{4D_{66}}{R^2}\{-nC_m(\frac{d\varphi}{dx}(x-a) + \varphi) - B_m\frac{d\varphi}{dx}\}^2]\, sin^2\,\omega\, t dx \end{aligned}$$

and

$$\begin{aligned} T = \frac{\rho_t R\omega^2}{2}\int_0^L [& A_m^2(\frac{d\varphi}{dx})^2 + B_m^2\varphi^2 + C_m^2\varphi^2(x \\ & - a)^2]\, cos^2\,\omega\, t\, dx \end{aligned} \tag{12}$$

With the help of these equation, many (or any) ring supports can be investigated. For minimum energy principal, the relation of strain energy U_{max} and kinetic energy T_{max} are obtained, i.e.

$$\begin{aligned} U\frac{\pi R}{2}\int_0^L \Bigg[& A_{11}A_m^2\left(\frac{d^2\varphi}{dx^2}\right)^2 + \frac{n^2 A_{22}}{R^2}B_m^2\varphi^2 \\ & + \frac{A_{22}}{R^2}C_m^2(x-a)^2\varphi^2 + \frac{2nA_{22}}{R^2}B_m C_m(x-a)\varphi^2 \\ & + \frac{2nA_{12}}{R}A_m B_m\varphi\frac{d^2\varphi}{dx^2} + \frac{2A_{12}}{R}A_m C_m(x-a)\varphi\frac{d^2\varphi}{dx^2} \\ & + A_{66}\left(B_m - \frac{n}{R}A_m\right)^2\left(\frac{d\varphi}{dx}\right)^2 - 2B_{11}A_m C_m(x-a)\left(\frac{d^2\varphi}{dx^2}\right)^2 \\ & - 4B_{11}A_m C_m\frac{d\varphi}{dx}\frac{d^2\varphi}{dx^2} + \frac{2n^2 B_{12}}{R^2}A_m C_m(x-a)\varphi\frac{d^2\varphi}{dx^2} \\ & + \frac{2nB_{12}}{R^2}A_m B_m\varphi\frac{d^2\varphi}{dx^2} - \frac{2nB_{12}}{R}B_m C_m(x-a)\varphi\frac{d^2\varphi}{dx^2} \\ & - \frac{4nB_{12}}{R}B_m C_m\varphi\frac{d\varphi}{dx} - \frac{2B_{12}}{R}C_m^2(x-a)^2\varphi\frac{d^2\varphi}{dx^2} \\ & - \frac{4B_{12}}{R}C_m^2(x-a)\varphi\frac{d\varphi}{dx} + \frac{2B_{22}}{R^3}(n^3 B_m C_m(x-a)\varphi^2 \\ & + n^2 B_m\varphi^2 + n^2 C_m^2(x-a)^2\varphi^2 + nB_m C_m(x-a)^2\varphi) \\ & + \frac{4B_{66}}{R}\Bigg[nB_m C_m\left(\frac{d\varphi}{dx}\right)^2(x-a) + nB_m C_m\varphi\frac{d\varphi}{dx} + B_m^2\left(\frac{d\varphi}{dx}\right)^2 \\ & - \frac{n^2}{R}A_m C_m\left(\frac{d\varphi}{dx}\right)^2(x-a) \\ & - \frac{n^2}{R}A_m C_m\varphi\frac{d\varphi}{dx} - \frac{n}{R}A_m B_m\left(\frac{d\varphi}{dx}\right)^2\Bigg] \\ & + D_{11}C_m^2\Bigg[\left(\frac{d^2\varphi}{dx^2}\right)^2(x-a)^2 + 4\left(\frac{d\varphi}{dx}\right)^2 + 4(x \\ & - a)\frac{d\varphi}{dx}\frac{d^2\varphi}{dx^2}\Bigg] + \frac{D_{22}}{R^4}\Big[n^4 C_m^2(x-a)^2\varphi^2 + n^2\varphi^2 B_m^2 \\ & + 2n^3 B_m C_m(x-a)\varphi^2\Big] - \frac{2D_{12}}{R^2}\Big[n^2 C_m^2\frac{d^2\varphi}{dx^2}(x-a)^2\varphi \\ & + nB_m C_m(x-a)\varphi\frac{d^2\varphi}{dx^2} + 2n^2 C_m^2(x-a)\varphi\frac{d\varphi}{dx} \\ & + 2nB_m C_m\varphi\frac{d\varphi}{dx}\Big] + \frac{4D_{66}}{R^2}\Big[n^2 C_m^2(x-a)^2\left(\frac{d\varphi}{dx}\right)^2 \\ & + n^2 C_m^2\varphi^2 + 2n^2 C_m^2\varphi\frac{d\varphi}{dx} + B_m^2\left(\frac{d\varphi}{dx}\right)^2 \\ & + 2nB_m C_m(x-a)\left(\frac{d\varphi}{dx}\right)^2 + 2nB_m C_m\varphi\frac{d\varphi}{dx}\Big]\Bigg] dx \end{aligned} \tag{13}$$

and

$$T\frac{\pi R\rho_t\omega^2}{2}\int_0^L \begin{bmatrix} A_m^2\left(\frac{d\varphi}{dx}\right)^2 \\ +B_m^2\varphi^2 + C_m^2\varphi^2(x-a)^2 \end{bmatrix}_{max} dx \tag{14}$$

Now, the Langrangian function can be written as:

$$\Pi = Tmax_{max}$$

The function is minimized with the help of vibration amplitudes A_m, B_m and C_m as:

$$\frac{\partial \Pi}{\partial A_m} = \frac{\partial \Pi}{\partial B_m} = \frac{\partial \Pi}{\partial C_m} = 0$$

The compact form for three equations is:

$$\begin{aligned}
&\left[A_{11}\int_0^L \left(\frac{d^2\varphi}{dx^2}\right)^2 dx + \frac{n^2 A_{66}}{R^2}\int_0^L \left(\frac{d\varphi}{dx}\right)^2 dx\right] A_m \\
&+\left[\frac{nA_{12}}{R}\int_0^L \varphi\frac{d^2\varphi}{dx^2}dx - \frac{nA_{66}}{R}\int_0^L \left(\frac{d\varphi}{dx}\right)^2 dx + \frac{nB_{12}}{R^2}\right. \\
&\left.\int_0^L \varphi\frac{d^2\varphi}{dx^2}dx - \frac{2nB_{66}}{R^2}\int_0^L \left(\frac{d\varphi}{dx}\right)^2 dx\right] B_m \\
&+\left[\frac{A_{12}}{R}\int_0^L (x-a)\varphi\frac{d^2\varphi}{dx^2}dx - B_{11}\int_0^L (x-a)\left(\frac{d^2\varphi}{dx^2}\right)^2 dx\right. \\
&-2B_{11}\int_0^L \left(\frac{d\varphi}{dx}\right)\left(\frac{d^2\varphi}{dx^2}\right)dx \\
&+\frac{n^2 B_{12}}{R^2}\int_0^L (x-a)\varphi\frac{d^2\varphi}{dx^2}dx - \frac{2n^2 B_{66}}{R^2}\int_0^L \left(\frac{d\varphi}{dx}\right)^2 (x \\
&-a)dx \\
&\left.-\frac{2n^2 B_{66}}{R^2}\int_0^L \varphi\frac{d\varphi}{dx}dx\right] C_m = \rho_t\omega^2\int_0^L \left(\frac{d\varphi}{dx}\right)^2 dx A_m
\end{aligned} \tag{15}$$

$$\begin{aligned}
&\left[\frac{nA_{12}}{R}\int_0^L \varphi\frac{d^2\varphi}{dx^2}dx - \frac{nA_{66}}{R}\int_0^L \left(\frac{d\varphi}{dx}\right)^2 dx + \right. \\
&\left.\frac{nB_{12}}{R^2}\int_0^L \varphi\frac{d^2\varphi}{dx^2}dx - \frac{2nB_{66}}{R}\int_0^L \left(\frac{d\varphi}{dx}\right)^2 dx\right] A_m + \left[\frac{n^2 A_{22}}{R^2}\right. \\
&\int_0^L \varphi^2 dx + A_{66}\int_0^L \left(\frac{d\varphi}{dx}\right)^2 dx + \frac{2n^2 B_{22}}{R^3}\int_0^L \varphi^2 dx \\
&\left.+\frac{4B_{66}}{R}\int_0^L \left(\frac{d\varphi}{dx}\right)^2 dx + \frac{n^2 D_{22}}{R^4}\int_0^L \varphi^2 dx + \frac{4D_{66}}{R^2}\int_0^L \left(\frac{d\varphi}{dx}\right)^2 dx\right] B_m \\
&+\left[\frac{nA_{22}}{R^2}\int_0^L (x-a)\,\phi^2 dx - \frac{nB_{12}}{R}\int_0^L (x-a)\,\varphi\frac{d^2\varphi}{dx^2}dx\right. \\
&-\frac{2nB_{12}}{R}\int_0^L \varphi\frac{d\varphi}{dx}dx + \frac{n^3 B_{22}}{R^3}\int_0^L (x-a)\,\varphi^2 dx \\
&+\frac{nB_{22}}{R^3}\int_0^L (x-a)\,\varphi^2 dx \\
&+\frac{2nB_{66}}{R}\int_0^L (x-a)\left(\frac{d\varphi}{dx}\right)^2 + \frac{2nB_{66}}{R}\int_0^L \varphi\frac{d\varphi}{dx}dx \\
&+\frac{n^3 D_{22}}{R^4}\int_0^L (x-a)\,\varphi^2 dx - \frac{nD_{12}}{R^2}\int_0^L (x-a)\,\phi\frac{d^2\varphi}{dx^2}dx \\
&-\frac{2nD_{12}}{R^2}\int_0^L \varphi\frac{d\varphi}{dx}dx + \frac{4nD_{66}}{R^2}\int_0^L (x-a)\left(\frac{d\varphi}{dx}\right)^2 dx \\
&\left.+\frac{4nD_{66}}{R^2}\int_0^L \varphi\frac{d\varphi}{dx}\right] C_m = \rho_t\omega^2\int_0^L \varphi^2 dx B_m
\end{aligned} \tag{16}$$

$$\begin{aligned}
&\left[\frac{A_{12}}{R}\int_0^L (x-a)\varphi\frac{d^2\varphi}{dx^2}dx - B_{11}\int_0^L (x-a)\left(\frac{d^2\varphi}{dx^2}\right)^2 dx\right. \\
&-2B_{11}\int_0^L \frac{d\varphi}{dx}\frac{d^2\varphi}{dx^2}dx + \frac{n^2 B_{12}}{R^2}\int_0^L (x-a)\varphi \\
&\frac{d^2\varphi}{dx^2}dx - \frac{2n^2 B_{66}}{R^2}\int_0^L (x-a)\left(\frac{d\varphi}{dx}\right)^2 dx - \\
&\left.\frac{2n^2 B_{66}}{R^2}\int_0^L \varphi\frac{d\varphi}{dx}dx\right] A_m + \left[\frac{nA_{22}}{R^2}\int_0^L (x-a)\varphi^2 dx - \frac{nB_{12}}{R}\right. \\
&\int_0^L (x-a)\varphi\frac{d^2\varphi}{dx^2}dx - \frac{2nB_{12}}{R}\int_0^L \varphi\frac{d\varphi}{dx}dx + \\
&\frac{n^3 B_{22}}{R^3}\int_0^L (x-a)\varphi^2 dx + \frac{nB_{22}}{R^3}\int_0^L (x-a)\varphi^2 dx + \frac{2nB_{66}}{R} \\
&\int_0^L (x-a)\left(\frac{d\varphi}{dx}\right)^2 dx + \frac{2nB_{66}}{R}\int_0^L \varphi\frac{d\varphi}{dx}dx + \\
&\frac{n^3 D_{22}}{R^4}\int_0^L (x-a)\varphi^2 dx - \frac{nD_{12}}{R^2}\int_0^L (x-a)\varphi\frac{d^2\varphi}{dx^2}dx \\
&-\frac{2nD_{12}}{R^2}\int_0^L \varphi\frac{d\varphi}{dx}dx + \frac{4nD_{66}}{R^2}\int_0^L (x-a)\left(\frac{d\varphi}{dx}\right)^2 dx + \\
&\frac{4nD_{66}}{R^2}\int_0^L \varphi\frac{d\varphi}{dx}dx\Big] B_m + \left[\frac{A_{22}}{R^2}\int_0^L (x-a)^2\,\varphi^2 dx\right. \\
&-\frac{2B_{12}}{R}\int_0^L (x-a)^2\varphi\frac{d^2\varphi}{dx^2}dx + \frac{4B_{12}}{R} \\
&\int_0^L (x-a)\varphi\frac{d\varphi}{dx} + \frac{2n^2 B_{22}}{R^3}\int_0^L (x-a)^2\varphi^2 dx \\
&\left.+ D_{11}\int_0^L (x-a)^2\left(\frac{d^2\varphi}{dx^2}\right)^2 dx\right. \\
&+4D_{11}\int_0^L \left(\frac{d\varphi}{dx}\right)^2 dx + 4D_{11}\int_0^L (x-a)\frac{d\varphi}{dx}\frac{d^2\varphi}{dx^2}dx \\
&+\frac{n^4 D_{22}}{R^4}\int_0^L (x-a)^2\varphi^2 dx - \frac{2n^2 D_{12}}{R^2} \\
&\int_0^L (x-a)^2\varphi\frac{d^2\varphi}{dx^2}dx - \frac{4n^2 D_{12}}{R^2}\int_0^L (x-a)\varphi\frac{d\varphi}{dx}dx \\
&+\frac{4n^2 D_{66}}{R^2}\int_0^L (x-a)^2\left(\frac{d\varphi}{dx}\right)^2 dx + \frac{4n^2 D_{66}}{R^2} \\
&\left.\int_0^L \varphi^2 dx + \frac{8n^2 D_{66}}{R^2}\int_0^L (x-a)\varphi\frac{d\varphi}{dx}dx\right] C_m \\
&= \rho_t\omega^2\int_0^L (x-a)^2\varphi^2 dx\, C_m
\end{aligned} \tag{17}$$

The above equations can be written in the form of matrices as:

$$\begin{bmatrix} a_{11} & a_{12} & a_{13} \\ a_{12} & a_{22} & a_{23} \\ a_{13} & a_{23} & a_{33} \end{bmatrix}\begin{bmatrix} A_m \\ B_m \\ C_m \end{bmatrix} = \rho_t\omega^2\begin{bmatrix} I_2 & 0 & 0 \\ 0 & I_9 & 0 \\ 0 & 0 & I_{11} \end{bmatrix} \tag{18}$$

The expressions for the terms $a_{ij}'s, I_2, I_9$ and I_{11} are given in appendix-I.

4. Annexation of fluid term

The acoustic wave equation represents pressure of sound in fluid and this equation of motion describing fluid is given by

$$\frac{1}{r}\frac{\partial}{\partial r}\left(r\frac{\partial\phi}{\partial r}\right) + \frac{1}{r^2}\frac{\partial^2\phi}{\partial\theta^2} + \frac{\partial^2\phi}{\partial x^2} = \frac{1}{c^2}\frac{\partial^2\phi}{\partial t^2} \tag{19}$$

where (x, θ, r) are the cylindrical coordinates and ϕ, t, c, r stands respectively, for acoustic pressure, time variable, fluid sound speeds and the axial coordinate adopted from the shell axis. The acoustic pressure expression for an immersed cylinder in a fluid that satisfied the acoustic wave Eq. (19), written in following form:

$$\phi = \phi_m\, sin(n\theta)H_n^{(2)}(k_r r)\psi(x)\, cos\,\omega\, t \tag{20}$$

Table 1 Convergence of RRM frequencies (Warburton 1965)

n	Method	m					
		1	2	3	4	5	6
2	(Warburton 1965)	2040.8	5637.6	8935.3	11405	13245	14775
	RRM	2043.7	5631.9	8926.4	11399.4	13243.7	14779.9
3	(Warburton 1965)	2199.3	4041.9	6620	9124	11357	13384
	RRM	2194.4	4031.2	6605.9	9108.4	11343.4	13374.9

where ϕ_m symbolizes the pressure amplitude, $H_n^{(2)}(k_r r)$ denotes the second kind of Hankel's functions with order *n*. The radial and axial wave numbers k_r and k_x respectively linked by the vector equation, $k_r = (k_0 - k_x)^{1/2}$, where $k_0 = \frac{w}{c}$ is written for the acoustic wave number of the fluid. Here k_r has many values and depends on the variablek_x. In order to ensure that the sound field fulfills the suitable conditions of radiation and decay as $r \to \infty$, the branch that meets the condition $k_r = \sqrt{k_0 - k_x}$ for $k_0 \geq k_r$ and $k_r = -i\sqrt{k_x - k_0}$ for $k_0 < k_x$, is chosen. For the assurance of keeping fluid connection with shell wall, the radial displacement of the fluid must be equal to that at the boundary of the outer wall of shell and the fluid.

The coupling condition is applied and is written as:

$$-\{1/(iw\phi_\rho)\}(\partial\phi/\partial r)|_{r=R} = (\partial w/\partial t)|_{r=R} \tag{21}$$

Subsequently the above condition has new form:

$$\phi_m = \left[\omega^2 \rho_f / k_r H_n^{'(2)}(k_r r)\right] C_m \tag{22}$$

where ρ_f signifies the fluid density and the dot written upon the $H_n^{(2)}(k_r r)$ represents the differentiation w.r.t the argument $k_r R$. With the application of the coupling condition (22) along with the relation (18), the shell frequency of the submerged CSs is given by as:

$$\begin{bmatrix} a_{11} & a_{12} & a_{13} \\ a_{12} & a_{22} & a_{23} \\ a_{13} & a_{23} & a_{33} + FL \end{bmatrix} \begin{bmatrix} A_m \\ B_m \\ C_m \end{bmatrix} = \rho_t \omega^2 \begin{bmatrix} I_2 & 0 & 0 \\ 0 & I_9 & 0 \\ 0 & 0 & I_{11} \end{bmatrix} \tag{23}$$

FL defines the fluid loading term and is written as:

$$FL = \Omega^2 (\rho_f/\rho_s)(R/h)(k_r R)^{-1}\left[H_n^{(2)}(k_r R) / H_n^{'(2)}(k_r R)\right] \tag{24}$$

When the fluid loaded term reduces to zero, the frequency equation fluid-filled cylindrical shells converts into that for the empty shell case.

5. Functionally graded material

The modeling of FG-CS is due to mixing two or more than two materials like ceramic and metal and the distribution of various functions and properties (physical and material), is termed as rule of mixture. Power law function has been utilized for with particular index using material properties in the thickness direction. The temperature and properties variations have been obtained by using the property of temperature and volume fraction. The distributions of volume fraction for all forms of CSs are assumed as (Chi and Chung 2006).

$$V_f = \left[\frac{z}{h} + \frac{1}{2}\right]^p \tag{25}$$

where *p*, *h* and z, respectively, denoted for power law index, thickness and the coordinate, where *z* which varies from zero to infinity.

A FG-CS consisting of two constituent materials. In these forms, nickel, stainless steel and zirconia are used for middle, internal and external surfaces, but their arrangement has profound influence on the formation of FG-CSs. If E_1 and E_2 as Young's moduli, ν_1 and ν_2 as Poisson's ratios, ρ_1 and ρ_2 mass densities respectively. Then effective material quantities for FG material are

$$\begin{aligned} E_{FGM} &= [E_1 - E_2]\left[\tfrac{2z+h}{2h}\right]^p + E_2, \\ \nu_{FGM} &= [\nu_1 - \nu_2]\left[\tfrac{2z+h}{2h}\right]^p + \nu_2, \\ \rho_{FGM} &= [\rho_1 - \rho_2]\left[\frac{2z+h}{2h}\right]^p + \rho_2 \end{aligned} \tag{26}$$

Toulokian *et al.* (1967) stated the material properties C at high temperature environ, with temperature-dependents which is a function of temperature. In Eq. (27), the constants ($C_0, C_{-1}, C_1, C_2, C_3$) are different for different material.

$$C = C_0(C_{-1}T^{-1} + C_1 T + C_2 T^2 + C_3 T^3) \tag{27}$$

6. Numerical results and discussion.

In this section, the versatile numerical technique RRM has been used in current study to investigate the vibration of fluid-filled FG-CS. For the convergence rate of CSs, the non-dimensional frequency enumerated in the current work, i.e., using RRM is happened to be in a good consistency. In Table 1, the frequencies (Hz) for a CSs are weighed against those calculated for a SS-SS end conditions by (Warburton 1965).

The frequencies are taken for circumferential modes *n* = 2, 3 and *m* = 1 ~ 6. There is once again comparison of empty and fluid-filled CSs with Gonclaves *et al*. (2006). The proposed model based on RRM can incorporate in order to accurately predict the acquired results of material data point. There is once again comparison of present results of CSs with Gonclaves *et al*. (1988), Goncalves and

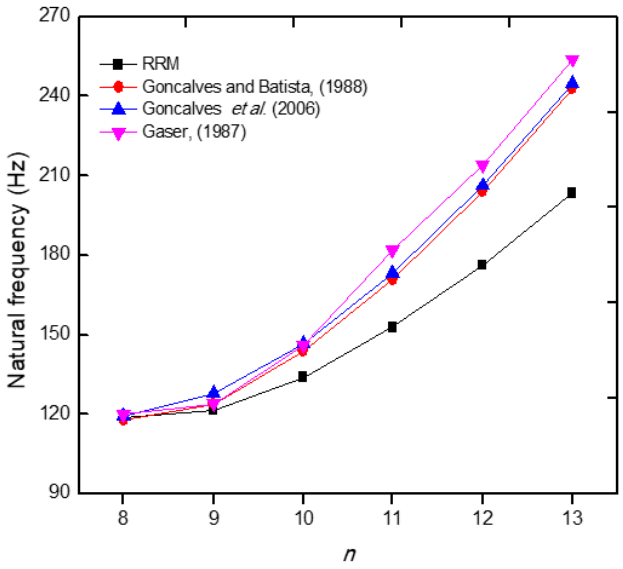

Fig. 2 Convergence of RRM frequencies (a) versus m (n= $1L=8$ in, h = 0.1 in, R = 2 in, $E = 30\times10^6$ lbf in^{-2},ν = 0.3, ρ = 7.35×10^{-4}lbf s^2 in^{-4})

Table 2 Comparison of fluid-filled and without fluid versus circumferential wave number

n	Without fluid	With fluid
1	13.548	6.9299
2	4.5920	1.9371
3	4.2633	2.0205
4	7.2250	3.7455
5	11.542	6.4292

Table 3 Comparison of fluid-filled and without fluid versus length-to-radius ratio

L/R	Without fluid	With fluid
0.2	439.36	210.57
1	87.331	34.386
5	16.917	7.4997
10	8.6035	4.1934
20	4.2633	2.2408

Table 4 Comparison of fluid-filled and without fluid versus height-to-radius ratio

h/R	Without fluid	With fluid
0.001	2.7919	1.3423
0.007	6.380	2.5217
0.01	7.9333	3.5103
0.03	13.557	6.5811
0.05	13.572	6.8545

Batista. (1988), Gasser (1987), as shown in Fig 2. The proposed model based on RRM can incorporate in order to accurately predict the acquired results of material data point. In Tables 2-4 shows the frequencies for fluid-filled and without fluid cylindrical shells with simply supported

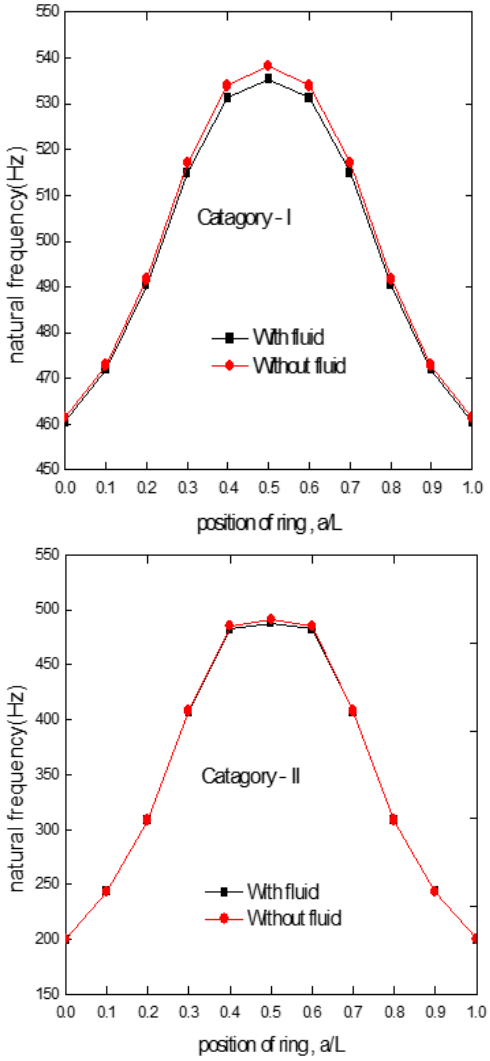

Fig. 3 Variations of frequencies versus the ring support a under various boundary conditions for FGM cylindrical shells (m = 1, n = 1, L = 20m, h = 0.002m, R = 1m, p = 0.5)

boundary condition. Table 2 indicates that the frequency values versus circumferential wave number. It is observed that the frequencies are highly visible for without fluid are higher than those for ones. They have been considerably reduced by the impact of terms. Table 3 represent frequencies with length-to-radius ratio using simply supported edge conditions. There is a pronounced decrease in frequencies when the cylindrical shell has been filled with fluid. Moreover it is observed that with increments in L/R, the fundamental frequencies increases.

Table 4 show the frequencies against thickness-to - radius ratios (h/R). As h/R is increased, the fundamental frequency increases for a fixed value of L/R. In these tables, the frequencies are considerably reduced when the shell are filled with fluid as compared to without fluid. They are approximately half of those for a cylindrical shell not filled with fluid. This reduction is approximately fifty percent. In Table 5, variations of natural frequencies (Hz) for cylindrical shells without and with ring supports are listed against circumferential wave number, n. The shells are

Table 5 Frequency versus wave number *n* with ring supports for empty and fluid-filled cylindrical shell

n	*a* = 0.1		*a* = 0.3		*a* =1	
	Empty	Fluid-filled	Empty	Fluid-filled	Empty	Fluid-filled
1	2269.12	1502.7	2463.22	1886.37	2231.65	1513.49
2	1735.94	1130.39	2143.98	1459.28	1649.77	1070.58
3	1436.13	936.26	2001.05	1364.64	1303.73	842.69
4	1296.79	846.06	1947.45	1329.97	1132.64	731.77
5	1235.14	806.27	1928.36	1317.63	1052.95	680.02
6	1207.46	788.57	1921.36	1313.21	1015.53	655.9
7	1194.43	780.11	1919.12	1311.68	997.38	644.61
8	1188.28	776.24	1918.82	1311.92	988.33	638.12
9	1185.47	774.41	1919.38	1312.48	983.81	635.37
10	1184.39	773.76	1920.35	1313.15	981.71	633.89

Table 6 Frequency versus wave number *m* with ring supports for empty and fluid-filled cylindrical shell

m	*a* = 0.1		*a* = 0.3		*a* = 0.5	
	Empty	Fluid-filled	Empty	Fluid-filled	Empty	Fluid-filled
1	2269.12	1501.93	2463.22	1886.36	2861.27	2861.27
2	2478.94	1552.99	2143.98	1953.15	2861.44	2861.44
3	3005.13	1344.18	2001.05	1806.77	2861.73	2861.73
4	4009.79	1223.62	1947.75	1737.35	2862.13	2862.13
5	5116.14	1169.19	1928.36	1703.94	2862.65	2862.65
6	6778.46	1145.16	1921.36	1686.88	2863.28	2863.28
7	7789.43	1133.98	1919.12	1679.46	2864.03	2780.61
8	8991.28	1128.68	1918.82	1677.73	2864.88	2575.17
9	9998.47	1125.58	1919.38	1682.04	2865.86	2440.89
10	1110.39	1123.82	1920.35	1689.25	2866.95	2440.37

submerged in the fluid. The ring supports are positioned at *a* = 0.1, 0.3, 1. The shell frequencies decrease as n is made to increase for each position of the ring support. The trend in decrements in frequency values goes down indefinitely with n. Moreover there is a visible tendency in shift of frequency due to addition of ring supports and their location points. Table 6 states variations of natural frequencies against the axial wave number, m for a cylindrical shell with ring supports positioned at *a* = 0.1, 0.3, 0.5 and is submerged in the fluid. An observation is made that values of the shell frequency increase indefinitely as values of m goes on increasing. Table 7 shows variations of natural frequencies (Hz) versus length to radius ratio (*L/R*) for a cylindrical shell with ring supports located at *a* = 0.3, 0.5, 1. The shell is immersed in a fluid. From the Table, it is noted that shell frequencies grow as *L/R* is enhanced i.e., as the shell becomes longer. In Table 8, natural frequencies (Hz) with thickness to radius (*h/R*) for a submerged cylindrical shell are demonstrated. The ring supports are situated at *a* = 0.3, 0.5, 1. With increase in values of *h/R*, the frequency increases fast in the beginning but gets slower as the shell gets thicker.

Table 9 shows frequencies against the ring position empty and fluid-filled cylindrical shells. It is found that first vibration frequencies increase as the positions of a ring support is shifted from *a* = 0~0.5 and they get highest values at *a* = 0.5. After this, they start to get lessened and at *a* = 1, coincide with those values that are observed at the initial position, *a* = 0 of a ring support. This behavior is noted for submerged and not submerged cases. So from the above data, it is noted that vibration frequencies are highly affected as the fluid factor and ring supports are added to the shell problem.

Fig. 3 depicts the frequency variations versus ring support for categories-I and-II cylindrical shells. These variations of frequencies are drawn with simply supported condition. As *a* is enhanced for these boundary conditions, the frequencies go up. At *a* (= 0.5) all the frequencies are higher and at *a* (= 0.6 ~ 0.9), the frequencies decreases. The frequencies are same at *a* = 0, 1 and rust itself a bell shape. These frequencies have a great impact on the vibration of FG-CSs. It is inferred this frequency behavior with position of the ring supports has paramount influence on the vibrations of FG-CSs.

Here frequencies of fluid-filled FG-CSs with ring supports are presented in following figures. The frequency variation with the position of the ring support at *a* = 0 ~ 1L for the simply supported edge conditions both categories as

Table 7 Frequency variations versus *L/R* with ring supports

L/R	*A = 0.3*	*A = 0.5*	*a = 1*
1	13.6	9.6	25.1
5	110.3	107.6	119.7
10	251.6	288.4	172.6
15	341.1	468.6	191.5
20	381.4	503.8	198.4

Table 8 Frequency variations versus *h/R* with ring supports

h/R	*a=0.3*	*a=0.5*	*a=1*
0.002	381.5	503.9918	198.5
0.005	401.7	503.9919	201.5
0.01	408.8	503.9920	202.6
0.02	412.4	503.9924	203.1
0.03	413.7	503.9931	203.3

Table 9 Frequency variations versus ring supports with empty and fluid-filled CSs

a	Empty	Fluid-Filled
0.0	2231.67	1477.93
0.1	2269.12	1502.7
0.2	2336.12	1547.09
0.3	2463.22	1631.27
0.4	2686.75	1779.31
0.5	2861.27	1894.88
0.6	2686.74	1779.29
0.7	2463.22	1631.27
0.8	2336.13	1547.11
0.9	2269.11	1502.72
10	2231.65	1477.91

shown in Fig 4. These figures depicts the frequency variations versus ring support for four forms of cylindrical shell with for three values of *law* exponent is p = 0.5, 1, 1.5. These variations of frequencies are drawn with the comparison of empty and fluid-filled cylindrical shell. As a is enhanced, the frequencies go up. At a (= 0.5L) all the frequencies are higher and at a (= 0.6L ~ 0.9L), the frequencies decreases. The frequencies are same at a = 0, 1L and rust itself a bell shape. It can be observed from these figure the fluid frequencies are lower than that of empty frequencies with category-I and-II. The reason of these frequency fluctuations is inducting the Hankel's function with fluid term. The frequency of category-I is higher than that of category-II. It is due to the material distribution of stainless steel and nickel. As we increase the fraction law exponent, the frequency increases for empty and fluid-filled shell with two categories. The fluid filled law exponents can be clearly seen lower down that of empty one. These frequencies have a great impact on the vibration of CSs. It is inferred this frequency behavior with position of the ring supports has paramount influence on the vibrations of FG-CSs.

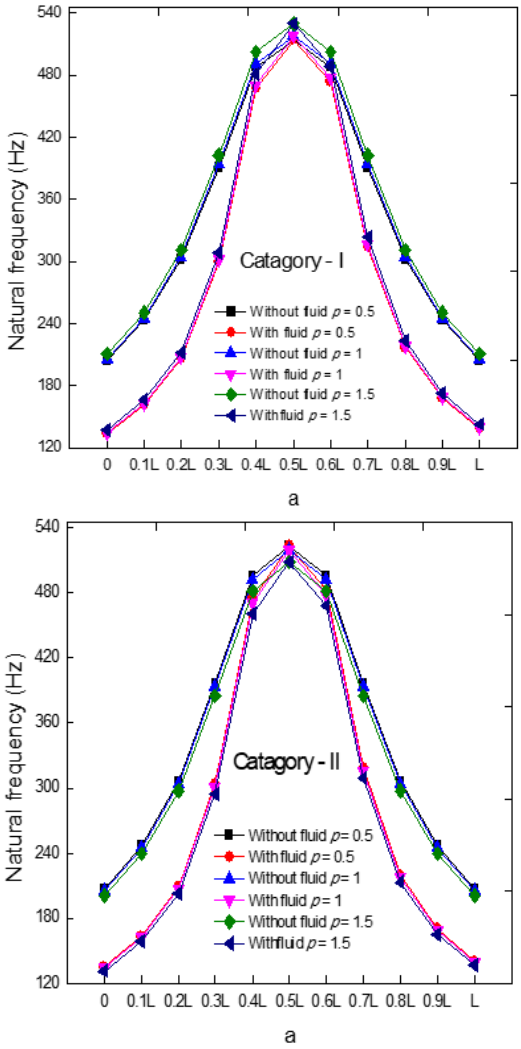

Fig. 4 Variation of natural frequencies (Hz) against the positions of the ring supports for without fluid and with fluid cylindrical shell (n =1, m =1, L= 8m, h = 0.004m, R=1m, E=2.1×10^{11} N/m^2, ν = *0.3*, ρ = 7850 Kg/m^3, ρ_f=1000 Kg/m^3)

7. Conclusions

In this analytical study, vibrations of fluid-filled functionally grade cylindrical shells have been investigated for the distribution of material composition of material with two categories of material. Here the Rayleigh-Ritz procedure has been applied to derive the shell frequency equation with fluid term. Hankel's functions of second kind are utilized to represent this phenomenon. The frequencies are higher for higher values of circumferential wave number. The problem is formulated by applying the Rayleigh-Ritz procedure and the shell fluid condition is annexed with the third equation of shell motion equations. These shells are stiffened by rings in the tangential direction. For isotropic materials, the physical properties are same everywhere where the laminated and functionally graded materials, they vary from point to point. The influence of the ring supports is investigated at various positions. Effect of ring supports with empty and fluid-

filled shell is presented using the Rayleigh - Ritz method with simply supported condition. The frequency behavior is investigated with empty and fluid-filled cylindrical shell with ring supports versus circumferential wave number and axial wave number. Also the variations have been plotted against the locations of ring supports for length-to-radius and height-to-radius ratio. Moreover, frequency pattern is found for the various position of ring supports for empty and fluid-filled cylindrical shell. The frequency first increases and gain maximum value with the increase of circumferential wave mode. It has been investigated that the frequencies lower down on implicating the fluid term. The shells are submerged in a fluid and terms describing fluid effects are added with the shell motion equations with ring supports. The longitudinal modal displacement functions are assessed by characteristic beam ones meet end conditions applied at the shell edges. Stability of a cylindrical shell depends highly on these aspects of material. More the shell material sustains a load due to physical situations, the more the shell is stable. Any predicted fatigue due to burden of vibrations is evaded by estimating their dynamical aspects. An extension of present study can be done for investigating the rotating FG-shells with ring supports.

Acknowledgements

The Authors extend their appreciation to the Deanship Scientific Research at King Khalid University for funding this work through large group Research Project under grant number: RGP2/388/45.

References

Akbaş Ş.D. (2017a), "Free vibration of edge cracked functionally graded microscale beams based on the modified couple stress theory", *Int. J. Struct. Stabil. Dyn.*, **17**(3), 1750033. https://doi.org/10.1142/S021945541750033X

Akbaş, Ş.D. (2016a), "Forced vibration analysis of viscoelastic nanobeams embedded in an elastic medium", *Smart Struct. Syst.*, **18**(6), 1125-1143. https://doi.org/10.12989/sss.2016.18.6.1125

Akbaş, Ş.D. (2016b), "Analytical solutions for static bending of edge cracked micro beams", *Struct. Eng. Mech.*, **59**(3), 579-599. https://doi.org/10.12989/sem.2016.59.3.579

Akbaş, Ş.D. (2017b), "Forced vibration analysis of functionally graded nanobeams", *Int. J. Appl. Mech.*, **9**(7), 1750100. https://doi.org/10.1142/S1758825117501009

Alwabli, A.S., Kaci, A., Bellifa, H., Bousahla, A.A., Tounsi, A., Alzahrani, D.A., Abulfaraj, A.A., Bourada, F., Benrahou, K.H., Tounsi, A., Mahmoud, S.R. and Hussain, M. (2021), "The nano scale buckling properties of isolated protein microtubules based on modified strain gradient theory and a new single variable trigonometric beam theory", *Adv. Nano Res.*, **10**(1), 15-24. https://doi.org/10.12989/anr.2021.10.1.015

Amabili, M., Pellicano, F. and Paidoussis M.P. (1998), "Nonlinear vibrations of simply Love, A.E.H. (1888), "On the small free vibrations and deformation of thin elastic shell", *Phil. Trans. R. Soc. London*, **A179**, 491-549. https://doi.org/10.1098/rsta.1888.0016.

Ansari, R. and Rouhi, H. (2015), "Nonlocal Flügge shell model for the axial buckling of single-walled Carbon nanotubes: An analytical approach", *Int. J. Nano Dimension*, **6**(5), 453-462. https://doi.org/10.7508/IJND.2015.05.002

Asghar, S. Hussain M, and Naeem M. (2019), "Non-local effect on the vibration analysis of double walled carbon nanotubes based on Donnell shell theory", *Physica E*, **116**, 113726. https://doi.org/10.1016/j.physe.2019.113726

Asghar, S., Khadimallah, M.A., Naeem, M.N., Ghamkhar, M., Khedher, K.M., Hussain, M., Bouzgarrou, S.M., Ali, Z., Mahmoud, S.R., Taj, M. and Tounsi, A. (2020b), "Small scale computational vibration of double-walled CNTs: Estimation of nonlocal shell model", *Adv. Concr. Constr.*, **10**(4), 345-355. https://doi.org/10.12989/acc.2020.10.4.34

Asghar, S., Naeem, M. N., Khadimallah, M. A., Hussain, M., Iqbal, Z. and Tounsi, A. (2020a), "Effect of chiral structure for free vibration of DWCNTs: Modal analysis", *Adv. Concr. Constr.*, **9**(6), 577-588. https://doi.org/10.12989/acc.2020.9.6.577

Avcar M. (2019), "Free vibration of imperfect sigmoid and power law functionally graded beams", *Steel Compos. Struct.*, **30**(6), 603-615. https://doi.org/10.12989/scs.2019.30.6.603

Benmansour, D.L., Kaci, A., Bousahla, A.A., Heireche, H., Tounsi, A., Alwabli, A.S., Alhebshi, A.M., Al-ghmady, K. and Mahmoud, S.R. (2019), "The nano scale bending and dynamic properties of isolated protein microtubules based on modified strain gradient theory", *Adv. Nano Res.*, **7**(6), 443. https://doi.org/10.12989/anr.2019.7.6.443

Cao, Q., Wang, R., Zhang, T., Wang, Y. and Wang, S. (2022), "Hydrodynamic modeling and parameter identification of a bionic underwater vehicle: RobDact", *Cyborg Bionic Syst.*, 2022. https://doi.org/10.34133/2022/9806328

Chi, S.H. and Chung, Y.L. (2006), "Mechanical behavior of functionally graded material plates under transverse load-part II: numerical results", *Int. J. Solids Struct.*, **43**, 3657-3691. https://doi.org/10.1016/j.ijsolstr.2005.04.010

Chung, H., Turula, P. Mulcahy, T.M. and Jendrzejczyk, J.A. (1981), "Analysis of cylindrical shell vibrating in a cylindrical fluid region", *Nuclear Eng. Des.*, **63**(1), 109-1012. https://doi.org/10.1016/0029-5493(81)90020-0.

Dang, V. H., Sedighi, H. M., Civalek, Ö. and Abouelregal, A. E. (2021), "Nonlinear vibration and stability of FG nanotubes conveying fluid via nonlocal strain gradient theory", *Struct. Eng. Mech.*, **78**(1), 103-116. https://doi.org/10.12989/sem.2021.78.1.103

Dong S.B. (1977), "A block-stodola eigen solution technique for large algebraic systems with non-symmetrical matrices", *Int. J. Numer. Meth. Eng.*, **11**, 247. https://doi.org/10.1002/nme.1620110204

Dong, Z., Li, X., Yamaguchi, H. and Yu, P. (2024), "Magnetic field effect on the sedimentation process of two non-magnetic particles inside a ferrofluid", *J. Magn. Magn. Mater.*, **589**, 171501. https://doi.org/10.1016/j.jmmm.2023.171501

Ebrahimi, F., Dabbagh, A., Rabczuk, T. and Tornabene, F. (2019), "Analysis of propagation characteristics of elastic waves in heterogeneous nanobeams employing a new two-step porosity-dependent homogenization scheme", *Adv. Nano Res.*, **7**(2), 135. https://doi.org/10.12989/anr.2019.7.2.135

Eltaher, M.A., Almalki, T.A., Ahmed, K.I. and Almitani, K.H. (2019), "Characterization and behaviors of single walled carbon nanotube by equivalent-continuum mechanics approach", *Adv. Nano Res.*, **7**(1), 39. https://doi.org/10.12989/anr.2019.7.1.039

Ergin, A. and Temarel, P. (2002), "Free vibration of a partially liquid-filled and submerged, horizontal cylindrical shell", *J. Sound Vib.*, **254**(5), 951-965. https://doi.org/10.1006/jsvi.2001.4139

Feng, J., Wang, W. and Zeng, H. (2024), "Integral sliding mode control for a class of nonlinear multi-agent systems with

multiple time-varying delays", *IEEE Access*, **12**, 10512-10520. https://doi.org/ 10.1109/ACCESS.2024.3354030

Fu, Y., Liu, Y., Wang, J., Wang, Y., Xu, G. and Wen, J. (2024), "Local resistance characteristics of elbows for supercritical pressure RP-3 flowing in serpentine micro-tubes", *Propuls. Power Res.*, In Press. https://doi.org/10.1016/j.jppr.2023.02.009

Fu, Z.H., Yang, B.J., Shan, M.L., Li, T., Zhu, Z.Y., Ma, C.P., Zhang, X., Gou, G.Q., Wang, Z.R. and Gao, W. (2020), "Hydrogen embrittlement behavior of SUS301L-MT stainless steel laser-arc hybrid welded joint localized zones", *Corros. Sci.*, **164**, 108337. https://doi.org/10.1016/j.corsci.2019.108337

Gasser LFF. (1987), "Free vibrations on thin cylindrical shells containing liquid", M.S. Thesis, Federal University of Rio de Janerio, Rio de Janerio:

Goncalves, P.B. and Batista (1988), "Non-linear vibration analysis of fluid-filled cylindrical shell", *J. Sound Vib.*, **127**(1), 133-143. https://doi.org/10.1006/jsvi.2001.4139

Gong, Q., Cai, M., Gong, Y., Chen, M., Zhu, T. and Liu, Q. (2024), "Grinding surface and subsurface stress load of nickel-based single crystal superalloy DD5", *Precis. Eng.*, **88**, 354-366. https://doi.org/10.1016/j.precisioneng.2024.02.017

Guo, J., Ding, B., Wang, Y. and Han, Y. (2023), "Co-optimization for hydrodynamic lubrication and leakage of V-shape textured bearings via linear weighting summation", *Physica Scripta*, **98**(12), 125218. https://doi.org/10.1088/1402-4896/ad07be

Han, Q., Li, X. and Chu, F. (2018), "Skidding behavior of cylindrical roller bearings under time-variable load conditions", *Int. J. Mech. Sci.*, **135**, 203-214. https://doi.org/10.1016/j.ijmecsci.2017.11.013

Iqbal, W., Jalil, M., Khadimallah, M.A., Ayed, H., Naeem, M.N., Hussain, M., Bouzgarrou, S.M., Mahmoud, S.R., Ghandourah, E., Taj, M. and Tounsi, A. (2020), "Runge-Kutta method for flow of dusty fluid along exponentially stretching cylinder", *Steel Compos. Struct.*, **36**(5), 603-615. https://doi.org/10.12989/scs.2020.36.5.603

Iqbal, W., Jalil, M., Khadimallah, M.A., Hussain, M., Naeem, M. N., Al Naim, A.F. and Tounsi, A. (2021), "Interaction of casson nanofluid with Brownian motion: Temperature profile with shooting method", *Adv. Nano Res.*, **10**(4), 349-357. https://doi.org/10.12989/anr.2021.10.4.349

Jiang, J. and Olson, M.D. (1994), "Vibrational analysis of orthogonally stiffened cylindrical shells using super elements", *J. Sound Vib.*, **173**, 73-83. https://doi.org/10.1006/jsvi.1994.1218

Khadimallah, M.A., Hussain, M., Khedher, K.M., Naeem, M.N. and Tounsi, A. (2020b), "Backward and forward rotating of FG ring support cylindrical shell", *Steel Compos. Struct.*, **37**(2), 137-150. https://doi.org/10.12989/scs.2020.37.2.137

Khadimallah, M.A., Safeer, M., Taj, M., Ayed, H., Hussain, M., Bouzgarrou, S.M., Mahmoud, S.R and Tounsi, A. (2020a), "The effects of the surrounding viscoelastic media on the buckling behavior of single microfilament within the cell: A mechanical model", *Adv. Concr. Constr.*, **10**(2), 141-149. https://doi.org/10.12989/acc.2020.10.2.141

Koizumi, M. (1997), "FGM Activities in Japan", *Compos. Part B Eng.*, **28**(1-2), 1-4. https://doi.org/10.1016/S1359-8368(96)00016-9

Kuang, W., Wang, H., Li, X., Zhang, J., Zhou, Q. and Zhao, Y. (2018), "Application of the thermodynamic extremal principle to diffusion-controlled phase transformations in Fe-C-X alloys: Modeling and applications", *Acta Materialia*, **159**, 16-30. https://doi.org/10.1016/j.actamat.2018.08.008

Lam, K.Y. and Loy, C.T. (1998), "Influence of boundary conditions for a thin laminated rotating cylindrical shell", *Compos. Struct.*, **41**, 215-228. https://doi.org/10.1016/S0263-8223(98)00012-9

Li, J., Wang, Z., Zhang, S., Lin, Y., Wang, L., Sun, C. and Tan, J. (2023), "A novelty mandrel supported thin-wall tube bending cross-section quality analysis: a diameter-adjustable multi-point contact mandrel", *Int. J. Adv. Manuf. Technol.*, **124**(11), 4615-4637. https://doi.org/10.1007/s00170-023-10838-y

Li, X., Yu, P., Niu, X., Yamaguchi, H. and Li, D. (2020), "Non-contact manipulation of nonmagnetic materials by using a uniform magnetic field: Experiment and simulation", *J. Magn. Magn. Mater.*, **497**, 165957. https://doi.org/10.1016/j.jmmm.2019.165957

Liu, W., Bai, X., Yang, H., Bao, R. and Liu, J. (2024), "Tendon driven bistable origami flexible gripper for high-speed adaptive grasping", *IEEE Robot. Auto. Lett.*, **9**(6). https://doi.org/10.1109/LRA.2024.3389413

Long, X., Chong, K., Su, Y., Du, L. and Zhang, G. (2023), "Connecting the macroscopic and mesoscopic properties of sintered silver nanoparticles by crystal plasticity finite element method", *Eng. Fract. Mech.*, **281**, 109137. https://doi.org/10.1016/j.engfracmech.2023.109137

Loy, C.T. and Lam, K.Y. (1997), "Vibration of cylindrical shells with ring supports", *J. Mech. Eng.*, **39**, 455-471. https://doi.org/10.1016/S0020-7403(96)00035-5

Mousavi, S.M., Rostami, M.N., Yousefi, M. and Dinarvand, S. (2021), "Dual solutions for MHD flow of a water-based TiO2-Cu hybrid nanofluid over a continuously moving thin needle in presence of thermal radiation", *Report Mech. Eng.*, **2**(1), 31-40. https://doi.org/10.31181/rme200102031m

Naeem, M.N., Ghamkhar, M., Arshad, S.H. and Shah, A.G. (2013), "Vibration analysis of submerged thin FGM cylindrical shells", *J. Mech. Sci. Technol.*, **27**(3), 649-656. https://doi.org/10.1007/s12206-013-0119-6

Najafizadeh, M.M. and Isvandzibaei, M.R. (2007), "Vibration of (FGM) cylindrical shells based on higher order shear deformation plate theory with ring support", *Acta Mechanica*, **191**, 75-91. https://doi.org/10.1007/s00707-006-0438-0

Safaei, B., Khoda, F.H. and Fattahi, A.M. (2019), "Non-classical plate model for single-layered graphene sheet for axial buckling", *Adv. Nano Res.*, **7**, 265-275. https://doi.org/10.12989/anr.2019.7.4.265

Sedighi, H.M. (2020), "Divergence and flutter instability of magneto-thermo-elastic C-BN hetero-nanotubes conveying fluid", *Acta Mechanica Sinica*, **36**, 381-396. https://link.springer.com/article/10.1007/s10409-019-00924-4

Sedighi, H.M., Ouakad, H.M., Dimitri, R. and Tornabene, F. (2020), "Stress-driven nonlocal elasticity for the instability analysis of fluid-conveying C-BN hybrid-nanotube in a magneto-thermal environment", *Physica Scripta*, **95**(6), 065204. https://doi.org/10.1088/1402-4896/ab793f

Sewall, J.L. and Naumann, E.C. (1968), *An Experimental and Analytical Vibration Study of Thin Cylindrical Shells with and without Longitudinal Stiffeners*, National Aeronautic and Space Administration.

Shah, A.G., Mahmood, T. and Naeem, M.N. (2009), "Vibrations of FGM thin cylindrical shells with exponential volume fraction law", *Appl. Math. Mech.*, **30**(5), 607-615. https://doi.org/10.1007/s10483-009-0507-x

Shahsavari, D., Karami, B. and Janghorban, M. (2019). "Size-dependent vibration analysis of laminated composite plates", *Adv. Nano Res.*, **7**(5), 337-349. https://doi.org/10.12989/anr.2019.7.5.337

Sharif, H., Naeem, M.N., Khadimallah, M.A., Ayed, H., Bouzgarrou, S.M., Al Naim, A.F., Muzamal, H. and Tounsi, A. (2020), "Energy effects on MHD flow of Eyring's nanofluid containing motile microorganism", *Adv. Concr. Constr.*, **10**(4), 357-367. https://doi.org/10.12989/acc.2020.10.4.357

Sharma, C.B. and Johns, D.J. (1971), "Vibration characteristics of a clamped-free and clamped-ring-stiffened circular cylindrical shell", *J. Sound Vib.*, **14**(4), 459-474.

https://doi.org/10.1016/0022-460X(71)90575-X
Sharma, P., Singh, R., & Hussain, M. (2019), "On modal analysis of axially functionally graded material beam under hygrothermal effect", *Proceedings of the Institution of Mechanical Engineers, Part C: Journal of Mechanical Engineering Science*, **234**(5), 1085-1101. https://doi.org/10.1177/0954406219888234.
Sobamowo, G.M., Ogunmola, B.Y. and Osheku, C.A. (2017), "Thermo-mechanical nonlinear vibration analysis of fluid-conveying structures subjected to different boundary conditions using Galerkin-Newton-Harmonic balancing method", *J. Appl. Comput. Mech.*, **3**(1), 60-79. https://doi.org/10.22055/JACM.2017.12620
Sodel W. (1981), *Vibration of Shell and Plates*, Mechanical Engineering Series, Marcel Dekker, New York, U.S.A.
Sofiyev, A.H. and Avcar, M. (2010), "The stability of cylindrical shells containing an FGM layer subjected to axial load on the pasternak foundation", *Engineering*, **2**, 228-236. https://doi.org/10.4236/eng.2010.24033
Sun, L., Liang, T., Zhang, C. and Chen, J. (2023), "The rheological performance of shear-thickening fluids based on carbon fiber and silica nanocomposite", *Phys. Fluids*, **35**(3), 32002. https://doi.org/10.1063/5.0138294
Sun, L., Wang, G. and Zhang, C. (2024), "Experimental investigation of a novel high performance multi-walled carbon nano-polyvinylpyrrolidone/silicon-based shear thickening fluid damper", *J. Intell. Mater. Syst. Struct.*, **35**(6), 661-672. https://doi.org/10.1177/1045389X23122299
Suresh, S. and Mortensen, A. (1997), "Functionally gradient metals and metal ceramic composites: Part 2 thermo mechanical behavior", *Int. Mater. Rev.*, **42**, 85-116. https://doi.org/10.1179/imr.1995.40.6.239
Taj, M., Khadimallah, M.A., Hussain, M., Khedher, K.M., Shamim, R.A., Ahmad, M. and Tounsi, A. (2020), "Analysis of nonlocal Kelvin's model for embedded microtubules: Via viscoelastic medium", *Smart Struct. Syst.*, **26**(6), 809-817. https://doi.org/10.12989/sss.2020.26.6.80
Taj, M., Khadimallah, M.A., Hussain, M., Mahmood, S., Safeer, M., Al Naim, A.F. and Ahmad, M. (2021), "Confinement effectiveness of Timoshenko and Euler Bernoulli theories on buckling of microfilaments", *Adv. Concr. Constr.*, **11**(1), 81-88. https://doi.org/10.12989/acc.2021.11.1.081
Toulokian YS. (1967), *Thermo Physical Properties of High Temperature Solid Materials*, Macmillan, New York, U.S.A.
Wang, C. M., Swaddiwudhipong, S. and Tian, J. (1997), "Ritz method for vibration analysis of cylindrical shells with ring-stiffeners", *J. Eng. Mech.*, **123**, 134-143. https://doi.org/10.1061/(ASCE)0733-9399(1997)123:2(134)
Wang, C., Wang, Z., Zhang, S., Liu, X. and Tan, J. (2023), "Reinforced quantum-behaved particle swarm-optimized neural network for cross-sectional distortion prediction of novel variable-diameter-die-formed metal bent tubes", *J. Comput. Des. Eng.*, **10**(3), 1060-1079. https://doi.org/10.1093/jcde/qwad037
Wang, W., Jin, Y., Mu, Y., Zhang, M. and Du, J. (2023a), "A novel tubular structure with negative Poisson's ratio based on gyroid-type triply periodic minimal surfaces", *Virtual Phys. Prototyp.*, **18**(1), e2203701. https://doi.org/10.1080/17452759.2023.2203701
Warburton, G.B. (1965), "Vibration of thin cylindrical shells", *J. Mech. Eng. Sci.*, **7**, 399-407. https://doi.org/10.1243/JMES_JOUR_1965_007_062_02
Wuite J, Adali S. (2005), "Deflection and stress behavior of nanocomposite reinforced beams using a multiscale analysis", *Compos. Struct.*, **71**(3-4), 388-396. https://doi.org/10.1016/j.compstruct.2005.09.011
Xiang, Y., Ma. Y.F., Kitipornchai. S., Lau. C.W.H. (2002), "Exact solutions for vibration of cylindrical shells with intermediate ring supports", *Int. J. Mech. Sci.*, **44**(9), 1907-1924. https://doi.org/10.1016/S0020-7403(02)00071-1
Xuebin, L. (2008), "Study on free vibration analysis of circular cylindrical shells using wave propagation", *J. Sound Vib.*, **311**, 667-682. https://doi.org/10.1016/j.jsv.2007.09.023
Yang, S., Zhang, Y., Sha, Z., Huang, Z., Wang, H., Wang, F. and Li, J. (2022b), "Deterministic manipulation of heat flow via three-dimensional-printed thermal meta-materials for multiple protection of critical components", *ACS Appl. Mater. Interf.*, **14**(34), 39354-39363. https://doi.org/10.1021/acsami.2c09602
Yang, W., Jiang, X., Tian, X., Hou, H. and Zhao, Y. (2023), "Phase-field simulation of nano-α′ precipitates under irradiation and dislocations", *J. Mater. Res. Technol.*, **22,** 1307-1321. https://doi.org/10.1016/j.jmrt.2022.11.165
Zhang, G., Yang, Z., Li, X., Deng, S., Liu, Y., Zhou, H., Peng, M., Fu, Z., Chen, R., Meng, D., Zhong, L., Zhou, Q. and Wei, S. (2024), "Gamma-ray irradiation induced dielectric loss of SiO_2/Si heterostructures in through-silicon vias (TSVs) by forming border traps", *ACS Appl. Electr. Mater.*, **6**(2), 1339-1346. https://doi.org/10.1021/acsaelm.3c01646
Zhang, X.M. (2002), "Parametric analysis of frequency of rotating laminated composite cylindrical shells with the wave propagation approach", *Comput. Meth. Appl. Mech. Eng.*, **191**, 2057-2071. https://doi.org/10.1016/S0045-7825(01)00368-1.
Zhu, Q., Chen, J., Gou, G., Chen, H. and Li, P. (2017), "Ameliorated longitudinal critically refracted—Attenuation velocity method for welding residual stress measurement", *J. Mater. Proc. Technol.*, **246**, 267-275. https://doi.org/10.1016/j.jmatprotec.2017.03.022
Zhu, S., Li, X., Bian, Y., Dai, N., Yong, J., Hu, Y., Li, J. and Chu, J. (2023), "Inclination-enabled generalized microfluid rectifiers via anisotropic slippery hollow tracks", *Adv. Mater. Technol.*, **8**(16), 2300267. https://doi.org/10.1002/admt.202300267

CC

Appendix

$$a_{11} = A_{11}I_1 + \frac{n^2A_{66}}{R^2}I_2$$

$$a_{12} = \frac{nA_{12}}{R}I_3 - \frac{nA_{66}}{R}I_2 + \frac{nB_{12}}{R^2}I_3 - \frac{2nB_{66}}{R^2}I_2$$

$$a_{13} = \frac{A_{12}}{R}I_4 - B_{11}I_5 - 2B_{11}I_6 + \frac{n^2B_{12}}{R^2}I_4 - \frac{2n^2B_{66}}{R^2}I_7 - \frac{2n^2B_{66}}{R^2}I_8$$

$$a_{22} = \frac{n^2A_{22}}{R^2}I_9 + A_{66}I_2 + \frac{2n^2B_{22}}{R^3}I_9 + \frac{4B_{66}}{R}I_2 + \frac{n^2D_{22}}{R^4}I_9 + \frac{4D_{66}}{R^2}I_2$$

$$a_{23} = \frac{nA_{22}}{R^2}I_{10} - \frac{nB_{12}}{R}I_4 - \frac{2nB_{12}}{R}I_8 + \frac{n^3B_{22}}{R^3}I_{10} + \frac{nB_{22}}{R^3}I_{10} + \frac{2nB_{66}}{R}I_7 + \frac{2nB_{66}}{R}I_8$$
$$+ \frac{n^3D_{22}}{R^4}I_{10} - \frac{nD_{12}}{R^2}I_4 - \frac{2nD_{12}}{R^2}I_8 + \frac{4nD_{66}}{R^2}I_7 + \frac{4nD_{66}}{R^2}I_8$$

$$a_{33} = \frac{A_{22}}{R^2}I_{11} - \frac{2B_{12}}{R}I_{12} - \frac{4B_{12}}{R}I_{13} + \frac{2n^2B_{22}}{R^3}I_{11} + D_{11}I_{14} + 4D_{11}I_2 + 4D_{11}I_{15}$$
$$+ \frac{n^4D_{22}}{R^4}I_{11} - \frac{2n^2D_{12}}{R^2}I_{12} - \frac{4n^2D_{12}}{R^2}I_{13} + \frac{4n^2D_{66}}{R^2}I_{16} + \frac{4n^2D_{66}}{R^2}I_9 + \frac{8n^2D_{66}}{R^2}I_{13}$$

where

$$I_1 = \int_0^L \left(\frac{d^2\varphi}{dx^2}\right)^2 dx$$

$$I_2 = \int_0^L \left(\frac{d\varphi}{dx}\right)^2 dx$$

$$I_3 = \int_0^L \varphi \frac{d^2\varphi}{dx^2} dx$$

$$I_4 = \int_0^L (x-a)\varphi \frac{d^2\varphi}{dx^2} dx$$

$$I_5 = \int_0^L (x-a)\left(\frac{d^2\varphi}{dx^2}\right)^2 dx$$

$$I_6 = \int_0^L \left(\frac{d\varphi}{dx}\right)\left(\frac{d^2\varphi}{dx^2}\right) dx$$

$$I_7 = \int_0^L (x-a)\left(\frac{d\varphi}{dx}\right)^2 dx$$

$$I_8 = \int_0^L \varphi \frac{d\varphi}{dx} dx$$

$$I_9 = \int_0^L \varphi^2 dx$$

$$I_{10} = \int_0^L (x-a)\varphi^2 dx$$

$$I_{11} = \int_0^L (x-a)^2\varphi^2 dx$$

$$I_{12} = \int_0^L (x-a)^2\varphi \frac{d^2\varphi}{dx^2} dx$$

$$I_{13} = \int_0^L (x-a)\varphi \frac{d\varphi}{dx} dx$$

$$I_{14} = \int_0^L (x-a)^2\left(\frac{d^2\varphi}{dx^2}\right)^2 dx$$

$$I_{15} = \int_0^L (x-a)\frac{d\varphi}{dx}\frac{d^2\varphi}{dx^2} dx$$

$$I_{16} = \int_0^L (x-a)^2\left(\frac{d\varphi}{dx}\right)^2 dx$$